Investigation on the fluctuation of hydraulic exciting force on a pump-turbine runner during the load rejection process

X L Fu[1], D Y Li[1, 2, 3, *], H J Wang[1, *], G H Zhang[1], X Z Wei[1, 4] and D Q Qin[1, 4]

[1] School of Energy Science and Engineering, Harbin Institute of Technology, Harbin, 150001, China
[2] State key Laboratory of Hydroscience and Engineering, Tsinghua University, Beijing, 100084, China
[3] Key Laboratory of Fluid and Power Machinery (Xihua University), Ministry of Education Sichuan, Chengdu, 610039, China
[4] State Key Laboratory of Hydro-Power Equipment, Harbin Institute of Large Electrical Machinery, Harbin, 150040, China

lideyou@hit.edu.cn, wanghongjie@hit.edu.cn

Abstract. The flow-induced vibration is one of the important reasons causing the instability of pump-turbines during the load rejection process. However, the flow mechanism is not clear. In this study, the load rejection process of a pump-turbine was investigated, considering the clearance between the runner and stationary parts, through three-dimensional turbulent flow simulation with the dynamic mesh technology. Unsteady pressure boundary conditions were established at the inlet of the spiral-casing and outlet of the draft tube. The rotational speed of runner was calculated through coupling the rigid body motion with the water flow. The simulated rotational speed of runner shows a good consistency with the corresponding experimental data. Based on the numerical results, the fluctuation of the hydraulic thrust and hydraulic torque on the runner and their formation mechanism were analysed. The results show that there exists complex flow in the draft tube and in the vaneless space during the load rejection process. The complex flow leads to the severe fluctuation of hydraulic thrust and hydraulic torque on the runner with a low frequency, which is about 0.06~0.4 times rated rotational frequency of the runner. Consequently, the hydraulic exciting source may induce intense vibration of the runner potentially.

1. Introduction

Nowadays, with the development of clean energy such as wind power and solar power, the pumped storage power generation technology as a regulating tool in the electric grid has developed rapidly [1-4]. In the process of regulating power grid, pump-turbines undergo frequent start-stop and conversion processes between different operating regimes [5]. The operating characteristics and internal flow of pump-turbines are quite complex during the transition processes [6, 7]. There often accompany intense vibrations of pumped storage units [8]. The load rejection process is such a complicated transition process, which the pumped storage units always experience during the operation process [9]. It is closely related to safe and stable operations of pumped storage units. Therefore, the stability and vibration of pump-turbines during the load rejection process should be considered in the design stage of pump-

turbines. In recent years, owing to the need of actual engineering, scholars have conducted a lot of studies on the load rejection process of pump-turbines.

The numerical calculation method on the transition processes of pump-turbines underwent a developing process which is from one-dimensional (1D) calculation method to three-dimensional (3D) calculation method, and then to the method of coupling 1D method with 3D method (1-3D). In early stage, 1D calculation method on the transition process of a pump-turbine is mainly the method of characteristic (MOC) [10]. The MOC is too simplified to offer fully detailed flow field distribution and non-linear characteristic of pressure pulsation which are used to optimize the pump-turbine and ensure the safe and stable operation of pump-turbines. Then, the fully 3D method was developed gradually [11, 12]. The fully 3D method could satisfy most requirements in the engineering in a certain sense. But this method still is not able to be widely applied in engineering under the limitation on the current computing capacity of computers. Comprehensively considering the advantages and disadvantages of 1D method and 3D method, a numerical calculation method of coupling 1D method with 3D method was proposed and developed. In this numerical method, the 1D equation which describes the transient flow in water conveyance pipelines and the Reynold-averaged Naiver Stokes equations which describe the incompressible turbulent flow in pump-turbines are solved simultaneously [13-18]. In order to further solve the problem that the MOC is inaccurate in the 1-3D method, Huang et al.[19] proposed an improved coupled method in which the results of the 1D are corrected with the 3D method. In contrast, Li et al. [20, 21] presented another numerical simulation method based on the experimental data of a dynamic transition process.

Coupling the aforementioned numerical simulation methods with experimental test, some research progresses on the dynamic instability of performances and pressure pulsation in the transition processes have been made. The relevant experimental tests show that there exists intense pressure pulsation in turbines during the transition processes [22-24]; the intense pressure pulsation is mainly caused by the rotor-stator interaction and the complex flow in turbines [25]. The hill chart of pump-turbines shows significant looping dynamic characteristic in the runaway process [26]. Zhang et al. [27, 28] analyzed the formation mechanism on the looping dynamic characteristic of pump-turbines in the runaway process with the numerical simulation method. Yin et al. [29] simulated the load rejection process and pointed out that the variation of the rotational speed is the direct factor which causes the dynamic instability of a pump-turbine. Liu et al. [30] analyzed the influence of inertia on the fluctuation of internal and performance characteristics in the runaway process. Fan et al. [31] pointed out that the fluctuation of hydraulic torque on the guide vane within a slight opening is caused by the repeating reversal of fluid in the guide vane region after load rejection. Nennemann et al. [32] investigated the effect of the stochastic dynamic load on the fatigue life of the runner. Xia et al. [33] investigated the correlation among the evolution of flow pattern in pump-turbines, dynamic pressure pulsation and hydraulic thrust on the runner, and found that the variation of discharge is the main reason for intense fluctuation of the hydraulic thrust on the runner in the runaway process.

So far, the existing 3D calculation methods on the transition process of hydraulic turbines have been relatively more mature compared with the previous calculation methods. However, the formation mechanisms of the dynamic instability of the performance characteristics and pressure pulsation are still not very clear. Especially, the formation mechanisms on the fluctuation of the hydraulic exciting force on the runner are more unclear during the load rejection process. Hence, the research gap was selected to investigate in this study.

In this study, firstly, the reasonable boundary conditions were determined according to the existing experimental data in the load rejection process. Next, the 3D turbulent flow in a pump-turbine during the load rejection process was simulated under considering the clearance between runner and stator. The simulated rotational speed of the runner was compared with the corresponding experimental data, the feasibility of predicting the actual load rejection process of a pump-turbine with the numerical simulation results was validated. Finally, the formation mechanisms on the fluctuation of the hydraulic exciting force on the runner during the load rejection process was analyzed according to the numerical

results with the method of coupling the time-frequency joint analysis and coherence analysis combining with the flow field.

2. Numerical Model and Computational Method

2.1. Computational domain

In this study, a pump-turbine in a pumped storage power plant was investigated. The pump-turbine includes a runner with 9 blades, 20 guide vanes, 20 stay vanes including a special one, a spiral casing and a draft tube. Nominal diameters of runner at inlet and outlet are 4850 mm and 2535 mm, respectively. The height of the guide vanes of the prototype pump-turbine is 425 mm. The size of the prototype is scaled to the size of model (1: 9.25). The nominal diameter of the model runner outlet is 274 mm.

The entire computational domain consists of the spiral-casing region, the stay vane region, the guide vane region, the runner region, the draft tube region and the clearance region between the runner and the stationary parts including the cover and the bottom ring as shown in figure 1 and 2.

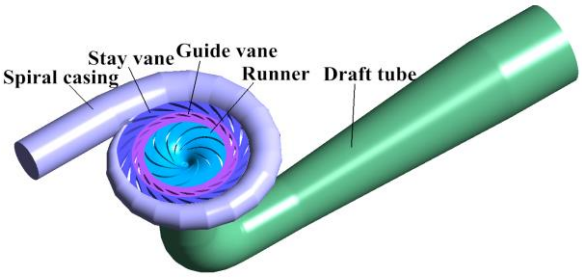

Figure 1. Computational domain.

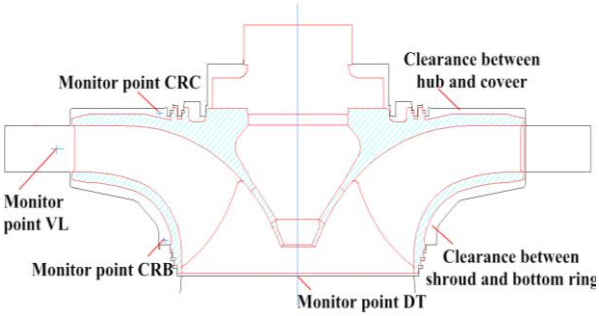

Figure 2. Clearance between the runner and the stationary parts and pressure monitoring points.

2.2. Mesh generation and mesh independency verification.

The structural grids were generated in all regions except the guide vane region. In order to simulate the dynamic closing process of the guide vane with the technology of dynamic mesh, the hybrid grids were generated in the guide vane region as shown in figure 3.

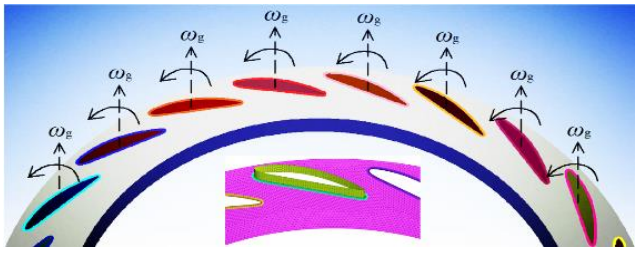

Figure 3. Grids of guide vane region and schematic diagram of closing guide vane.

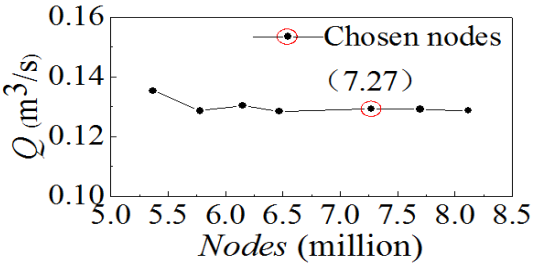

Figure 4. Mesh independency verification (Discharge).

In this study, seven sets of grids were generated in the computational domain with a 25 mm guide vane opening. The number of nodes is increasing from five million to eight million. The relationship between discharge and the number of nodes is shown in figure 4. Comprehensively considering the accuracy and calculation time of the numerical simulation, the mesh with 7.27 million nodes was selected to simulate the transient flow in a pump-turbine during the load rejection process.

2.3. Boundary conditions.

The unsteady total pressure and static pressure boundary conditions were respectively determined at the spiral-casing inlet and the draft tube outlet as shown in figure 5 and 6. The outflow boundary condition was set at the outlet of the clearance between the hub and the cover.

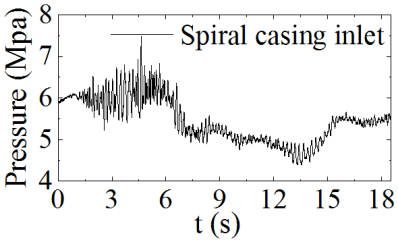

Figure 5. Unsteady total pressure at the spiral casing inlet.

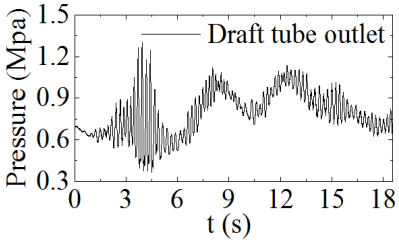

Figure 6. Unsteady static pressure at the draft tube outlet.

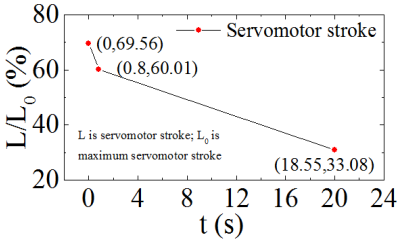

Figure 7. Closing law of the guide vanes during the load rejection process.

During the load rejection, the guide vane was closing gradually as shown in figure 3. The closing law of the guide vanes during the load rejection process is shown in figure 7. The dynamic closing process of the guide vane was simulated with the technology of dynamic mesh in FLUENT software.

During the load rejection process, the rotational speed of runner was calculated according to the equations (1) - (2) using the method of coupling of the rigid body motion with the water flow through a user defined function (UDF) in the FLUENT software.

$$M = J\frac{d\omega}{dt} \tag{1}$$

$$\omega_{i+1} = \omega_i + \frac{M_i}{J}(t_{i+1} - t_i) \tag{2}$$

where M denotes the resultant torque on the rotor; J denotes the inertia of the rotor; ω denotes the angular speed of the rotor, t denotes the time. Subscripts 'i' and 'i+1' respectively denote i_{th} and $i_{\text{th+1}}$ time step.

2.4. Numerical scheme and solve control

In this study, the RNG k-ε turbulent model was selected to close the Reynolds-averaged governing equations. The turbulent flow in a pump-turbine was simulated with the commercial calculation software FLUENT. In the numerical simulation, the second-order upwind scheme was selected to discretize the convective term. The first-order upwind scheme was adopted to discretize turbulent kinetic energy, turbulent dissipation term. The discrete algebraic equations were solved with the SIMPLEC algorithm. The residual of physical quantities in the numerical calculation is 10^{-5}. The time step of the unsteady computation is 0.0012 s. The maximum iterations are 25 in each time step. In this study, the transient flow in a pump-turbine during the load rejection process was initialized with the steady numerical result of the critical condition point where the pump-turbine just enters into the load rejection process.

3. Results and Discussion

3.1. The verification of the numerical results

In order to verify the correctness of the numerical results of the transient flow during the load rejection process, the unit rotational speed was compared with the experimental data as shown in figure 8. The relative rotational speed is defined as equation (3).

$$n_r = \frac{n}{n_0} \times 100\% \tag{3}$$

where n_r denotes the relative rotational speed, n denotes the rotational speed, n_0 denotes the rotational speed at the initial instant of the load rejection process. It can be seen from figure 8, the rotational speed obtained from simulation is basically consistent with the experimental data on the overall trend. In addition, the maximum relative runaway speed of simulation is 126.47%, while the corresponding experimental value is 128.17%. The difference is only 1.70% between the simulation and experiments. It indicates that the numerical result of the transient flow is reasonable in a certain error range.

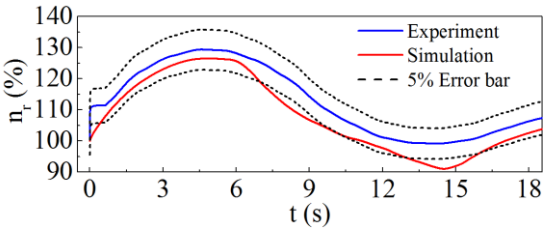

Figure 8. Comparison of rotational speed between simulation and experiments.

3.2. Analysis of hydraulic thrust on runner

In order to analyse the vibration of runner during the load rejection process, the hydraulic thrust on the runner including its radial component, axial component and torque are shown in figures 9~12.

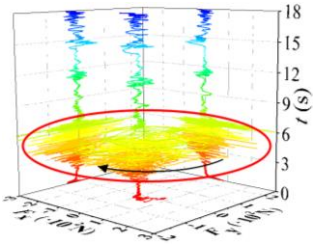

Figure 9. Variation of radial hydraulic thrust including F_x and F_y on runner with time

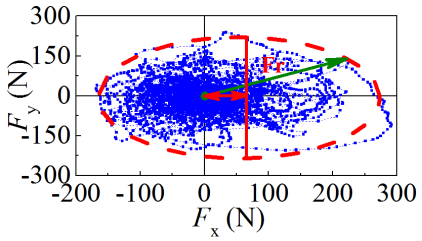

Figure 10. Distributing trajectory of radial hydraulic thrust on runner

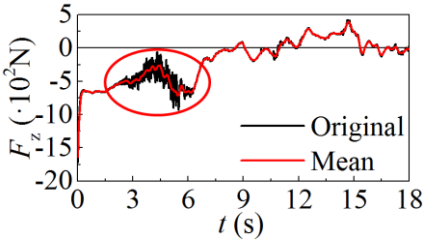

Figure 11. Variation of axial hydraulic thrust on the runner with time.

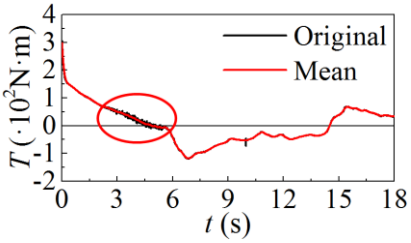

Figure 12. Variation of hydraulic torque on the runner with time.

Figures 9, 11 and 12 show that the hydraulic thrust and hydraulic torque on runner fluctuate intensely near the point of the first runaway condition (t= 4.8 s). Meanwhile the figures 9 and 10 show that the distributing trajectory of radial hydraulic thrust on runner seriously deviates from the center of the runner. It indicates that there exists intense flow-induced vibration of runner.

In order to determine the flow-induced vibrational frequency of runner, the analysis method of short time Fourier transform (STFT) was used to analyze the radial hydraulic thrust, axial hydraulic thrust and hydraulic torque on runner as shown in figures 13~16 (f_0 is the rated frequency of runner at initial instant of load rejection process).

It can be seen that the fluctuating intensity of various frequency components near the point of the first runaway condition (t= 4.8 s) is higher than the corresponding intensity at other instants. Additionally, the fluctuating intensity of the lower frequency components is higher than the fluctuating intensity of the high frequency components. There are similar distributing characteristics near the instants (t=11 s, 15 s, and 18 s) with near the instant (t= 4.8 s). Moreover, there also exist blade passing frequency and its corresponding harmonic frequencies in figures 13~16.

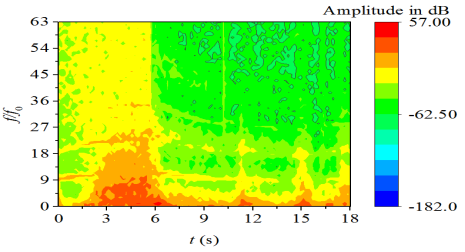

Figure 13. STFT result of radial hydraulic thrust F_x on the runner.

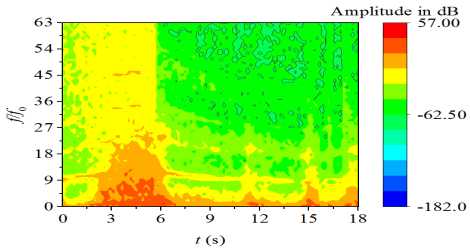

Figure 14. STFT result of radial hydraulic thrust F_y on the runner

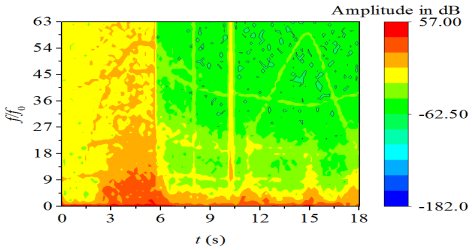

Figure 15. STFT result of axial hydraulic thrust F_z on the runner.

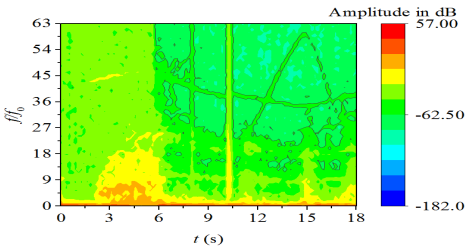

Figure 16. STFT result of hydraulic torque T on the runner.

In order to distinguish the lower frequency components, the analysis method of continuous wavelet transform (CWT) was adopted to analyse the lower frequency components of the hydraulic thrust and hydraulic torque on runner as shown in Figures 17-20 (f_0 is the rated frequency of the runner at initial instant of load rejection process). It is clear that the fluctuating intensity of the low frequency components of the axial hydraulic thrust F_z on runner is stronger than the corresponding fluctuating intensity of radial hydraulic thrust F_x, F_y and hydraulic torque on the runner. The stronger low frequency fluctuating components are about 0.06~0.4f_0.

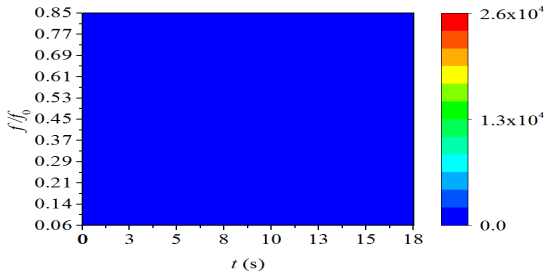

Figure 17. CWT result of radial hydraulic thrust F_x on runner.

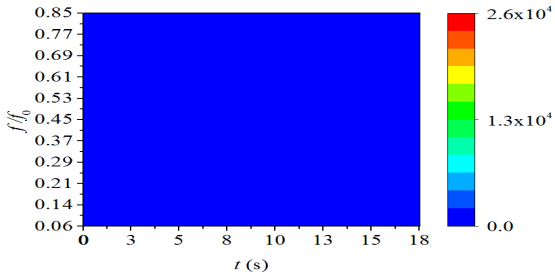

Figure 18. CWT result of radial hydraulic thrust F_y on runner.

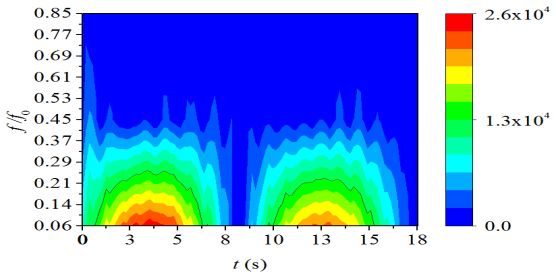

Figure 19. CWT result of axial hydraulic thrust F_z on runner.

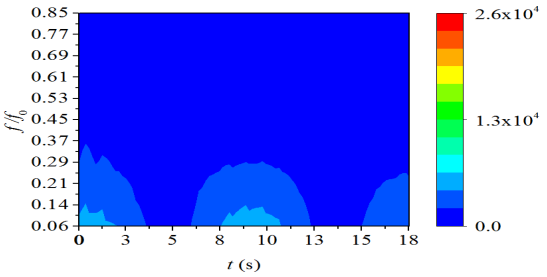

Figure 20. CWT result of hydraulic torque T on runner.

3.3. Analysis of hydraulic pressure near runner

The hydraulic pressure near runner is closely related to the fluctuation of hydraulic thrust on the runner. The monitor points of pressure are arranged near the runner as shown in figure 2. In the meridian plane through the center of the outlet of draft tube, VL is the monitor point in vaneless space, DT is the monitor point at the inlet of draft tube, CRC is the monitor point in the clearance between the runner and the cover, CRB is the monitor point in the clearance between the runner and the bottom ring. The results of STFT on the pressure signal are shown in Figures 21~24 (f_0 is the rated frequency of runner at initial instant of load rejection process).

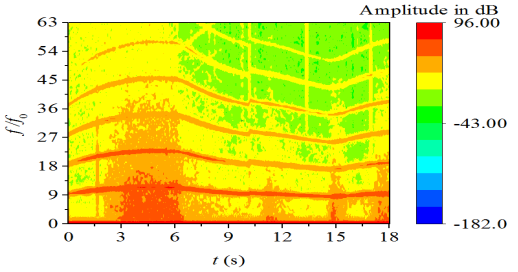

Figure 21. STFT result of pressure at monitor point VL

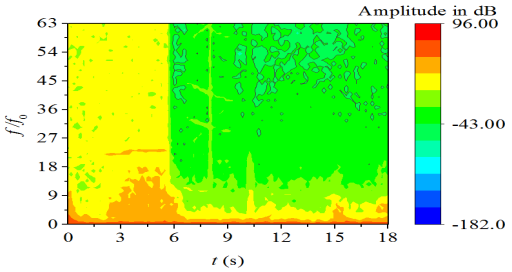

Figure 22. STFT result of pressure at monitor point DT

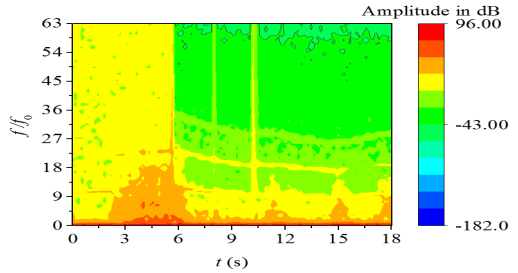

Figure 23. STFT result of pressure at monitor point CRC.

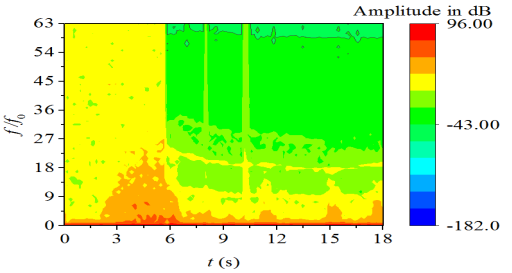

Figure 24. STFT result of pressure at monitor point CRB.

Comparing the STFT results of the pressure signal with the STFT results of the hydraulic thrust on the runner in figures 13~16, it can be seen that almost all the time-frequency characteristics of the pressure signals at each monitor points are generally similar with the time-frequency characteristics of the hydraulic thrusts on runner. It indicates that the vibration of runner are related to the fluctuation of pressure near the runner during the load rejection process. However, there are no quite significant difference among the pressure signals at monitor points VL, DT, CRC and CRB except the fluctuating intensity of pressure signal at VL, which is obviously stronger than others. Thus, it is not clear which pressure signal concretely causes the fluctuation of various hydraulic thrusts on the runner.

3.4. Coherence analysis among hydraulic thrusts on runner and pressure

In order to determine which pressure signal concretely causes the fluctuation of various hydraulic thrusts on runner, the method of coherence analysis is applied to discuss the relationship among the hydraulic thrusts and pressure signals as shown in figures 25~28 (f_0 is the rated frequency of runner at initial instant of load rejection process). Figure 25 and Figure 26 show the radial hydraulic thrust F_x and F_y are mainly related to the pressure at VL, CRC and CRB. Figures 27 and 28 show that the axial hydraulic thrust F_z and hydraulic torque T on the runner are mainly related to the pressure at DT.

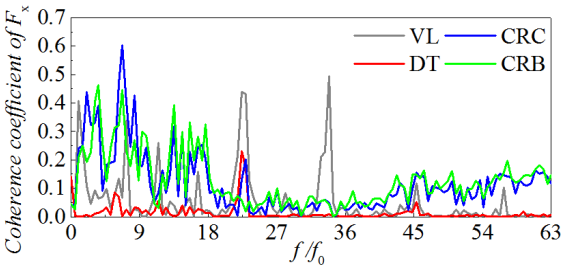

Figure 25. Coherence analysis among the radial hydraulic thrust F_x and the pressure signals at VL, DT, CRC and CRB

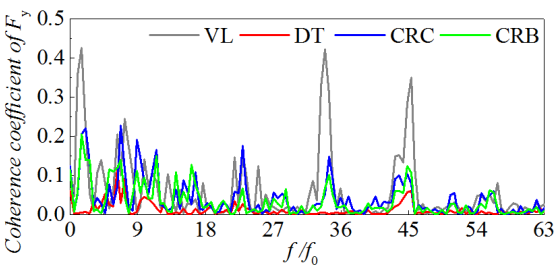

Figure 26. Coherence analysis among the radial hydraulic thrust F_y and the pressure signals at VL, DT, CRC and CRB.

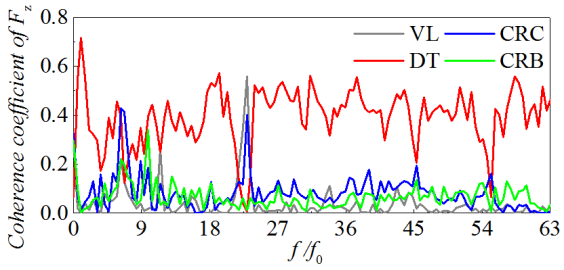

Figure 27. Coherence analysis among the axial hydraulic thrust F_z and the pressure signals at VL, DT, CRC and CRB

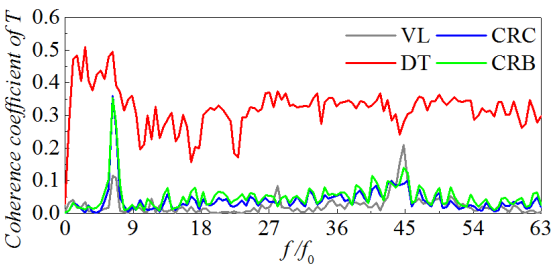

Figure 28. Coherence analysis among the hydraulic torque T and the pressure signals at VL, DT, CRC and CRB

3.5. Flow mechanism analysis on the fluctuation of hydraulic exciting force

In order to further analyse the flow mechanism which causes the radial hydraulic thrust on runner and the pressure in the vaneless space fluctuating intensely, the surface streamline in the vaneless space was extracted as shown in figure 29.

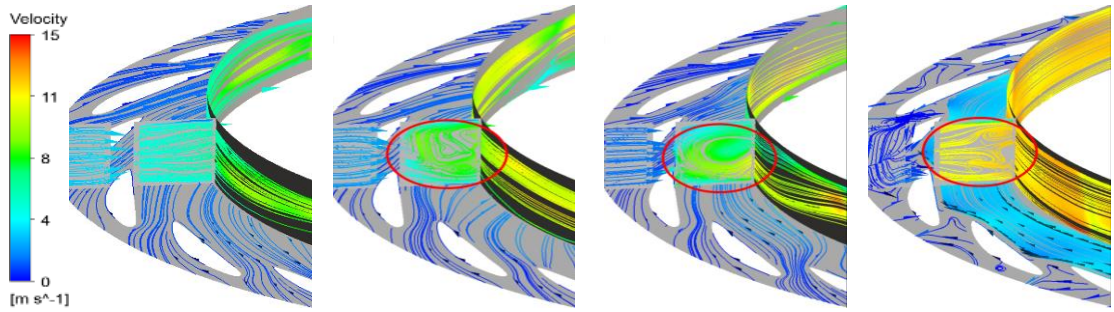

(a) t= 3.0 s (b) t= 4.8 s (c) t= 5.76 s (d) t= 6.72 s

Figure 29. Surface streamlines on three different surfaces in the vaneless space

At the instant (t= 3 s), the surface streamline in the vaneless space is very smooth. However, at instants (t= 4.8 s and 5.76 s), there appear obvious vortex flow in the vaneless space. Hence, the radial hydraulic thrust on runner and pressure in the vaneless space fluctuate intensely near the point of the first runaway condition (t= 4.8 s).

Adopting the similar analysis method with above mentioned method in figure 29, the surface streamline in draft tube was extracted as shown in figure 30. At all instants (t= 3.0 s, 4.8 s, 5.76 s and 6.72 s) during the load rejection process, there exist significant back-flow in the draft tube. The back-flow in the draft tube directly impacts the surface of runner. So the axial hydraulic thrust and hydraulic torque on runner are closely related to the flow in draft tube. In addition, at the instants (t= 3.0 s, 4.8 s and 5.76 s), there are obvious vortex flow in the draft tube. Therefore, the axial hydraulic thrust and hydraulic torque on runner fluctuate intensely near the point of the first runaway condition (t= 4.8 s).

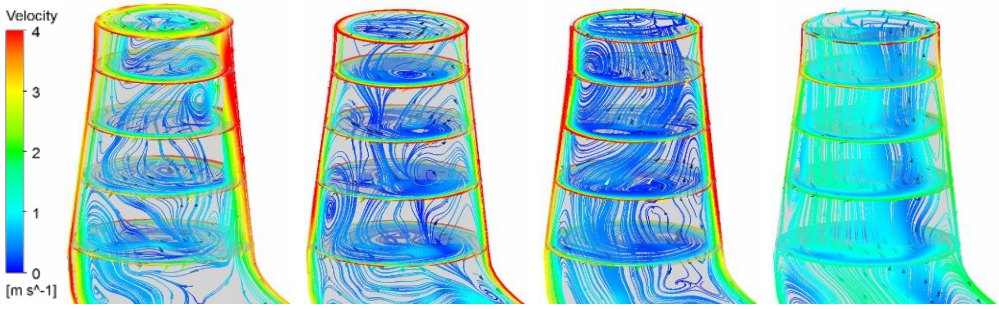

(a) t= 3.0 s (b) t= 4.8 s (c) t= 5.76 s (d) t= 6.72 s

Figure 30. Surface streamline on six different surfaces in the draft tube

4. Conclusions

In this study, the 3-D transient load rejection process of a pump-turbine was simulated. The simulated rotational speed of runner shows a good consistency with the experimental data. According to simulated results, the fluctuation of hydraulic thrust, hydraulic torque on the runner and underlying flow mechanism were analysed. Some conclusions are obtained as following.

During the load rejection process, the hydraulic thrust and hydraulic torque on the runner fluctuate intensely with low frequency (The low frequencies are about 0.06~0.4 times rated rotational frequency of the runner), which may cause the serious vibration of the runner and even threaten the safe and stability of the pump-turbine potentially.

The fluctuation of axial hydraulic thrust and hydraulic torque on the runner is mainly related to the pressure pulsation at the inlet of draft tube; While the fluctuation of radial hydraulic thrust is mainly related to the pressure pulsation in the vaneless space and in the clearance between the runner and stationary parts.

The fluctuation of axial hydraulic thrust and hydraulic torque on runner is caused by the back-flow and vortex flow in the draft tube. The fluctuation of radial hydraulic thrust on the runner is caused by the vortex flow in the vaneless space. Therefore, the flow-induced vibration of the runner is mainly caused by the complex flow in the draft tube and in the vaneless space during the load rejection process. It means that it is possible to decrease the flow-induced vibration of runner through controlling the flow in the draft tube and in the vaneless space during the load rejection process.

Acknowledgement

This work was supported by Open Research Fund Program of State Key Laboratory of Hydroscience and Engineering (Grant No. sklhse-2018-E-02) and Open Fund of Key Laboratory of Fluid and Power Machinery (Xihua Uninversity), Ministry of Education Sichuan (Grant No. szjj-2017-100-1-001).

References

[1] Zhang Y, and Wu Y 2016 A review of rotating stall in reversible pump turbine Proceedings of the

Institution of Mechanical Engineers, Part C: Journal of Mechanical Engineering Science 231 1181-1204
[2] Li D, Wang H, Qin Y, Han L, Wei X, and Qin D 2017 Entropy production analysis of hysteresis characteristic of a pump-turbine model Energy Conversion & Management 149 175-191
[3] Li D, Wang H, Qin Y, Wei X, and Qin D 2018 Numerical simulation of hysteresis characteristic in the hump region of a pump-turbine model Renewable Energy 115 433-447
[4] Li D Y, Gong R Z, Wang H J, Wei X Z, Liu Z S and Qin D Q 2016 Unstable head-flow characteristics of pump-turbine under different guide vane openings in pump mode Journal of Drainage and Irrigation Machinery Engineering 1 1-8 (in Chinese)
[5] Li D, Han L, Wang H, Gong R, Wei X, and Qin D 2017 Flow characteristics prediction in pump mode of a pump turbine using large eddy simulation Archive Proceedings of the Institution of Mechanical Engineers Part E Journal of Process Mechanical Engineering 231 961-977
[6] Zhang Y, Liu K, Xian H, and Du X 2017 A review of methods for vortex identification in hydroturbines Renewable and Sustainable Energy Reviews
[7] Li Q F, Liu M M, Liu Q, Zhang Z and Zhang J X 2017 Analysis of forces on runner and blades of pump-turbine under braking condition Journal of Drainage and Irrigation Machinery Engineering 7 588-595 (in Chinese)
[8] Zhang Y, Chen T, Li J, and Yu J 2017 Experimental study of load variations on pressure fluctuations in a prototype reversible pump turbine in generating mode ASME Journal of Fluids Engineering 139 74501
[9] Zhang F, Fu J, Fan Y L and Zhou X J 2017 Main shaft run-out research of hydraulic generator unit in load rejection process based on empirical mode decomposition Journal of Drainage and Irrigation Machinery Engineering 10 863-868 (in Chinese)
[10] Walseth E, Nielsen T, and Svingen B 2016 Measuring the dynamic characteristics of a low specific speed pump—turbine model Energies 9 199
[11] Zhang L, and Zhou D 2013 CFD research on runaway transient of pumped storage power station caused by pumping power failure IOP Conf. Series: Materials Science and Engineering 52 52027
[12] Liu J 2011 Numerical simulation of the transient flow in a radial flow pump during stopping period ASME Journal of Fluids Engineering 133 111101
[13] [Ruprecht A, Helmrich T, Aschenbrenner T, and Scherer T 2002 Simulation of vortex rope in a turbine draft tube Proceedings of the Hydraulic Machinery and Systems 21st IAHR Symposium (Lausanne, Switzerland)
[14] Cherny S, Chirkov D, Bannikov D, Lapin V, Skorospelov V, Eshkunova I, and Avdushenko A 2010 3D numerical simulation of transient processes in hydraulic turbines IOP Conf. Series: Earth and Environmental Science 12 12071
[15] Avdyushenko A Y, Cherny S G, Chirkov D V, Skorospelov V A, and Turuk P A 2013 Numerical simulation of transient processes in hydroturbines Thermophysics and Aeromechanics 20 577-593
[16] Nicolle J, Morissette J F, and Giroux A M 2012 Transient CFD simulation of a Francis turbine startup IOP Conf. Series: Earth and Environmental Science 15 62014
[17] Nicolle J, Giroux A M, and Morissette J F 2014 CFD configurations for hydraulic turbine startup IOP Conf. Series: Earth and Environmental Science 22 32021
[18] Zhang X, and Cheng Y 2012 Simulation of hydraulic transients in hydropower systems using the 1-D-3-D coupling approach Journal of Hydrodynamics, Ser. B 24 595-604
[19] Huang W, Fan H, and Chen N 2012 Transient simulation of hydropower station with consideration of three-dimensional unsteady flow in turbine IOP Conf. Series: Earth and Environmental Science 15 52003
[20] Li Z, Bi H L, Wang Z, and Yao Z 2016 Three-dimensional simulation of unsteady flows in a pump-turbine during start-up transient up to speed no-load condition in generating mode Proceedings of the Institution of Mechanical Engineers Part A Journal of Power & Energy 230 570-585

[21] Li Z, Bi H, Karney B, Wang Z, and Yao Z 2017 Three-dimensional transient simulation of a prototype pump-turbine during normal turbine shutdown Journal of Hydraulic Research 55 520-537
[22] Trivedi C, Cervantes M J, Gandhi B K, and Dahlhaug O G 2014 Transient pressure measurements on a high head model Francis turbine during emergency shutdown, total load rejection, and runaway ASME Journal of Fluids Engineering 136 1-18
[23] Trivedi C, Cervantes M J, Bhupendrakumar G, and Dahlhaug O G 2014 Pressure measurements on a high-head Francis turbine during load acceptance and rejection Journal of Hydraulic Research 52 283-297
[24] Trivedi C, Gandhi B K, Cervantes M J, and Dahlhaug O G 2015 Experimental investigations of a model Francis turbine during shutdown at synchronous speed Renewable Energy 83 828-836
[25] Houde S, Fraser R, Ciocan G, and Deschênes C 2012 Experimental study of the pressure fluctuations on propeller turbine runner blades: part 2, transient conditions IOP Conf. Series: Earth and Environmental Science 15 62061
[26] Zeng W, Yang J, Hu J, and Tang R 2017 Effects of pump-turbine S-shaped characteristics on transient behaviours: experimental investigation Journal of Physics: Conference Series 813 12056
[27] Zhang X, Cheng Y, Xia L, and Yang J 2014 Dynamic characteristics of a pump-turbine during hydraulic transients of a model pumped-storage system: 3D CFD simulation IOP Conf. Series: Earth and Environmental Science 22 32030
[28] Zhang X, Cheng Y, Xia L, Yang J, and Qian Z 2016 Looping dynamic characteristics of a pump-turbine in the S-shaped region during runaway ASME Journal of Fluids Engineering 138 91102
[29] Yin J, WANG D, WALTERS K, and Wei X 2014 Investigation of the unstable flow phenomenon in a pump turbine Science China Physics, Mechanics & Astronomy 57 1119-1127
[30] Liu J, Liu S, Sun Y, Zuo Z, Wu Y, and Wang L 2012 Instability study of a pump-turbine at no load opening based on turbulence model IOP Conf. Series: Earth and Environmental Science 15 2035
[31] Fan H, Yang H, Li F, and Chen N 2014 Hydraulic torque on the guide vane within the slight opening of pump turbine in turbine operating mode IOP Conference Series: Earth and Environmental Science 22 32050
[32] Nennemann B, Morissette J F, Chamberlandlauzon J, Monette C, Braun O, Melot M, Coutu A, Nicolle J, and Giroux A M 2014 Challenges in dynamic pressure and stress predictions at no-load operation in hydraulic turbines IOP Conf. Series: Earth and Environmental Science 22 32055
[33] Xia L, Cheng Y, Yang Z, You J, Yang J, and Qian Z 2017 Evolutions of pressure fluctuations and runner loads during runaway processes of a pump-turbine Journal of Fluids Engineering 139 091101.